ELSEVIER

Biochimica et Biophysica Acta 1364 (1998) 55–62

BIOCHIMICA ET BIOPHYSICA ACTA
BBA

# Angular dependence of electron paramagnetic resonances of an azide–NO complex of cytochrome *c* oxidase: orientation of the haem–copper axis in cytochrome $aa_3$ from ox heart

Dominic J.B. Hunter [a], John C. Salerno [b], W. John Ingledew [a,*]

[a] *School of Biological and Medical Sciences, University of St. Andrews, St. Andrews, Fife, Scotland, KY16 9AL, UK*
[b] *Department of Biology, Rensselaer Polytechnic Institute, Troy, NY 12180, USA*

Received 3 June 1997; revised 7 January 1998; accepted 14 January 1998

**Abstract**

The orientation dependence of the EPR signals arising from the azide–nitric oxide complex of cytochrome oxidase was investigated using oriented multilayers of mitochondrial membranes from ox heart. Variations in line shape of the $\Delta M_S = 1$ signal of the triplet state were apparent, whilst the $\Delta M_S = 2$ transitions between $g = 4.7$ and 3.9 varied in intensity as the angle of the applied magnetic field was varied. These half-field signals were maximal with the field parallel to the membrane plane. A model of the bi-liganded azide–nitric oxide complex has been constructed, in which the nitric oxide is bound to the high-spin haem in a bent configuration, with the Fe–N=O plane at 60–90° to the membrane plane and the azide bound to the copper, distal from the haem. In addition, angular variations of the signals at $g' = 11$ and $g'$ around 3.5, derived from an integer–spin complex, were also observed. © 1998 Elsevier Science B.V.

*Keywords:* Cytochrome oxidase; EPR; Orientation

## 1. Introduction

Mitochondrial cytochrome *c* oxidase (ferrocytochrome *c*: oxygen oxidoreductase, EC 1.9.3.1) terminates the respiratory chain. The enzyme catalyses the reduction of oxygen to water by ferrous cytochrome *c* concomitant with the extrusion of protons from the mitochondrial matrix. The structure and function of this important enzyme has been extensively investigated using a wide variety of techniques and recently preliminary details of a crystal structure have been published [1,2]. The enzyme contains four redox active centres; cytochromes *a* and $a_3$ and coppers $Cu_A$ and $Cu_B$. The haem *a* in cytochrome *a* is six-coordinate and always low-spin, $Cu_A$ is comprised of two closely associated copper atoms [3]. These two centres are involved in accepting and transferring electrons from cytochrome *c* to the catalytic centre of the enzyme. The catalytic core of the enzyme is formed by cytochrome $a_3$ (five-coordinate haem *a*, which is high-spin in the absence of exogenous ligands) and $Cu_B$ (a single copper atom); this site is the location of oxygen binding and reduction

Abbreviations: EPR: electron paramagnetic resonance; $H_0$: applied magnetic field; $H_{rf}$, r.f. field: magnetic field associated with incident microwave radiation

* Corresponding author. Fax: +44-1334-463400; E-mail: wji@st-and.ac.uk


*PII* S0005-2728(98)00006-1

and is probably intimately involved in the vectorial translocation of protons by the enzyme.

The electron paramagnetic resonance spectrum (EPR) of cytochrome *c* oxidase (cytochrome $aa_3$) reflects these arrangements. A low spin signal is observed arising from Fe(III) haem *a*, and the bi-copper $Cu_A$ centre gives rise to an unusual signal close to $g = 2$. In the oxidised enzyme, the catalytic core of the enzyme is usually EPR-silent, due to anti-ferromagnetic coupling between the haem $a_3$ ($Fe^{3+}$, $S = 5/2$) and the $Cu_B^{2+}$ ($S = 1/2$) which gives rise to an integer–spin (probably $S = 2$) system [4].

Preceding resolution of the structure by X-ray crystallography the sequences of many cytochrome *c* oxidases had been determined and biophysical studies, combined with site-directed mutagenesis, had provided a remarkably accurate picture of the catalytic core of the enzyme. Subunit I binds the haems and $Cu_B$, whilst subunit II binds $Cu_A$. Bacterial quinol oxidases do not possess $Cu_A$ and subunit II from these oxidases has lost those residues which ligand the copper, though the overall sequence of the subunit has notable areas of conservation [5].

Models of the region around the binuclear Fe–Cu centre were proposed [6,7] which have been confirmed and better resolved by the X-ray crystal structures. In the mammalian enzyme, the two haems lie on opposite sides of transmembrane helix X, at an angle of 104° to each other. They are liganded by histidine 61 from helix II and histidine 378 from helix X (haem *a*) and histidine 376 from helix X (haem $a_3$) (bovine numbering). $Cu_B$ lies close to the five-coordinate high-spin haem $a_3$, liganded by histidine residues 240, from helix VI and 290 and 291 from between helices VII and VIII [1].

The resolved crystal structure confirms the orientation of the haem groups within cytochrome *c* oxidase determined by EPR studies using oriented multilayers of mitochondrial membranes [8]. The haem normal ($g_z$) of cytochrome *a* lies in the plane of the membrane, whilst the $g_x$ and $g_y$ resonances are oriented at 60° and 30° to the membrane normal respectively. These resonances correspond to the in-haem-plane projections of the $d_{xz}$ and $d_{yx}$ orbitals and so approximate to the axes of highest and lowest unpaired electron density. The orientation of the $g = 6$ signal from high-spin haem (Fe(III)–Cu(I)) shows that this haem is also oriented with its normal in the membrane plane and that both haems lie between the transmembrane helices like ‘dinner plates between skittles’.

The structure and function of the haem–copper oxidases have been probed extensively using the binding of extrinsic ligands to the catalytic centre of the enzymes. Some forms of the enzyme give rise to diagnostic but not well-characterised EPR resonances. Nitric oxide (NO) is a ligand of special interest since it resembles dioxygen, but possesses an unpaired electron, allowing it to transform an EPR-undetectable even electron state into an odd electron state which can be studied by EPR. Reaction of reduced cytochrome $aa_3$ with nitric oxide produces a classic ferrous–haem–NO ($S = 1/2$) EPR spectrum. Reaction of oxidised cytochrome $aa_3$ with nitric oxide alone produces a high-spin haem EPR signal from cytochrome $a_3$, probably as a result of disruption of the antiferromagnetic coupling between cytochrome $a_3^{3+}$ and cupric $Cu_B$ [9,10]. When azide reacts with the fully oxidised enzyme the initial effect is to produce integer–spin signals and a shift in the Soret band consistent with a high-spin compound. Subsequently a low-spin haem spectrum is developed. In the high-spin compound the azide may be bound to the copper centre, leakage of electrons into the inhibited enzyme then reduces the copper and the azide binds to the haem, causing it to become low-spin [11,12].

In the presence of both NO and azide a bi-ligand state with a different set of resonances is observed. Although formed from the oxidised enzyme, it is probably one electron more reduced, and of the form $Fe(II) \cdot NO–N_3H \cdot Cu(II)$ as discussed by Stevens et al. [9]. This complex displays EPR signals characteristic of a triplet ($S = 1$) state with a small zero-field splitting, with a broad transition from $g = 2.6$ extending through the $g = 2$ region to $g = 1.69$ and a half-field transition at $g = 4.3$ ($\Delta M_s = 2$) showing hyperfine splitting due to the copper. These sharp features around $g = 4.3$ correspond to $\Delta M_s = 2$ transitions within the triplet state formed by the interaction of the ferrohaem $a_3$–NO complex ($S = 1/2$) and the cupric $Cu_B$–azide complex ($S = 1/2$). In purified cytochrome *c* oxidase, this triplet signal consists of features at $g = 4.7$, 4.4 and 4.0 [9]. Analogous signals have been observed in other oxidases [12]. Other signals from nitric oxide in frozen solution and from

copper and free radicals obscure parts of the $\Delta M_s = 1$ signal from the triplet in the $g = 2$ region. Since azide and nitric oxide form a complex with both elements of the binuclear centre of cytochrome $aa_3$ whose final state is probably $Fe^{2+}$–NO/$Cu_B^{2+}$–$N_3H$, the angular variation of the signals from this complex should give information on the nature of the triplet state and the arrangement of the components contributing to it. This paper investigates the orientation dependence of EPR spectroscopic features of the azide–NO complex of mitochondrial cytochrome *c* oxidase and hence the spatial relationship of the binuclear centre components of this enzyme.

## 2. Materials and methods

### *2.1. Preparation of mitochondrial membrane fragments*

Mitochondria (heavy mitochondrial fraction) were prepared from ox heart muscle [13] and were disrupted by a single passage through a French pressure cell as described previously [14].

### *2.2. Oriented multilayers*

Mitochondrial membrane fragments, suspended to approximately 15 mg protein/ml in 2 mM HEPES, pH 7.4, were incubated with 100 mM sodium azide (BDH, 'Analar' grade) for 1 h at 0°C. Oriented multilayers were then prepared by depositing the treated French-press membranes onto nitrocellulose-coated acetate sheet by centrifugation in a swinging bucket rotor (Beckman SW28) at $50\,000 \times g$ for 1 h at 4°C. Hemispherical polycarbonate inserts were used to produce a flat internal bottom to the centrifuge tube. The deposited membranes were dried under a gentle stream of nitrogen for up to 1 to 3 h. This procedure has been used extensively to produce oriented multilayer samples for optical and EPR spectroscopy and low-angle X-ray studies [8,15–18]. Samples produced in this way typically contain 25% water by weight and cytochrome oxidase retains 75–80% of its activity [17,18].

The multilayers were then sliced into strips and inserted into quartz EPR tubes of approximately 3 mm internal diameter. The multilayers were then made anaerobic by three cycles of evacuation (0.1 atm) and flushing with oxygen-free nitrogen (BOC) before exposure to nitric oxide for 20 min [9]. The EPR tubes were then quickly frozen and stored under liquid nitrogen until use.

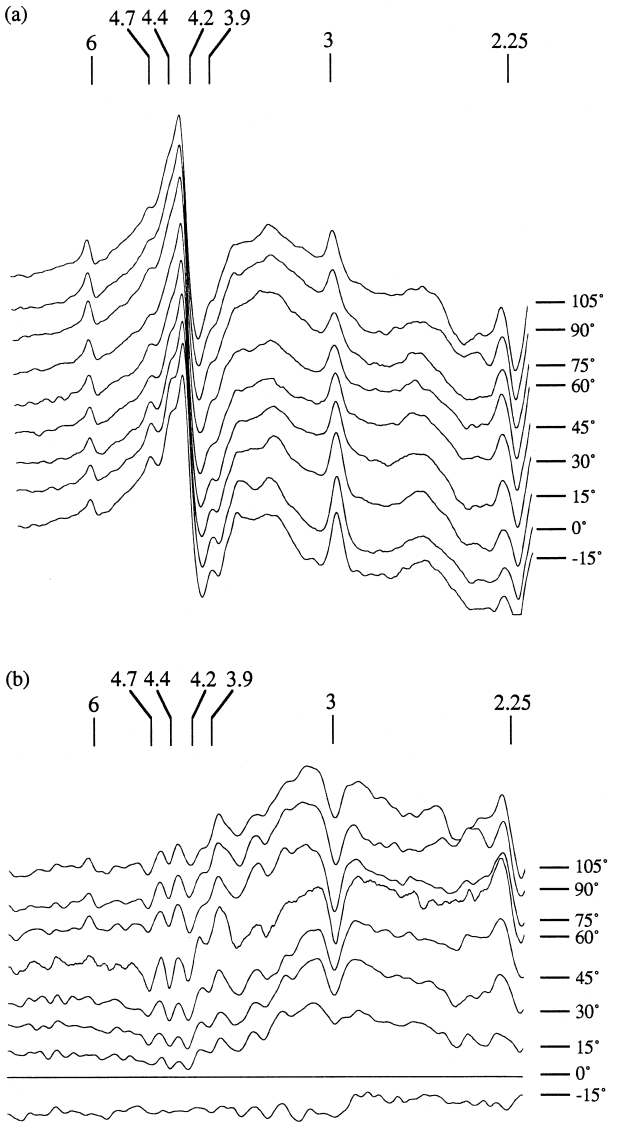


Fig. 1. (a) EPR spectra of oriented multilayers prepared from mitochondrial membranes and treated with azide and nitric oxide, recorded with the applied magnetic field at angles between −15° and 105° to the membrane plane. The *g* values of the major resonances are shown above the spectra. EPR spectrometer conditions were: modulation amplitude 4 G, microwave power 20 mW, frequency 9.45 GHz, temperature 14 K. (b) EPR difference spectra of the azide–NO treated multilayers. Each spectrum is that at *X*° minus the spectrum at 0°. Spectrometer conditions were as in (a).

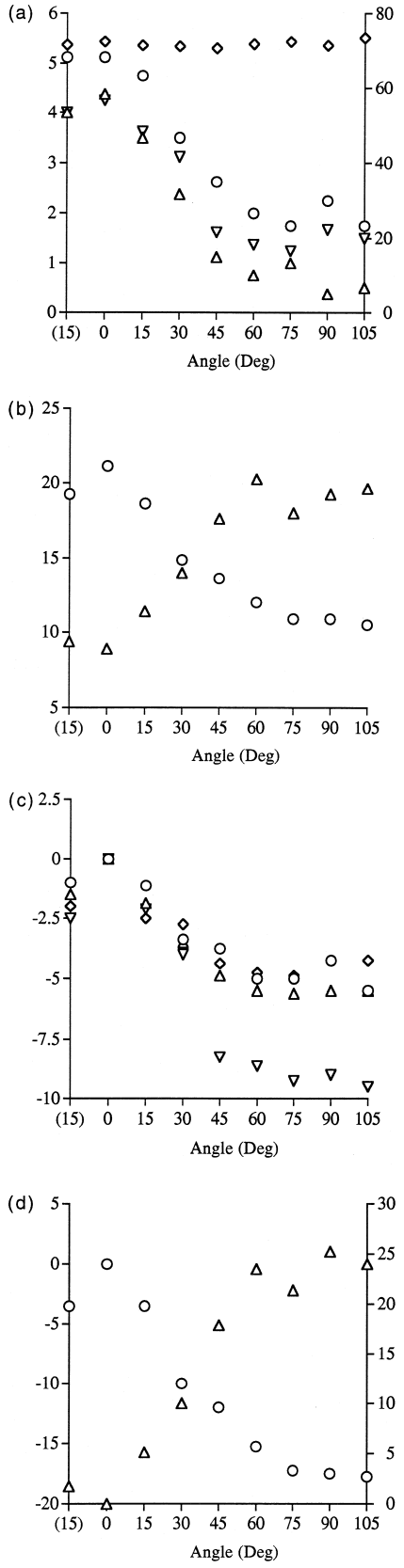


Fig. 2. Angular variation of the intensities of the EPR signals of interest. All points are the means of four spectral determinations: the range of the S.E.M. for each curve is noted. (a) Azide–NO signals at $g = 4.7$ (○) (S.E.M range 0.13–0.73), $g = 4.4$ (△) (0.21–0.64), $g = 4.2$ (◇) (8.80–10.50) and $g = 3.9$ (▽) (0.41–0.78). (b) Resonances at $g = 3$ (○) (1.60–3.20) and $g = 2.25$ (△) (1.70–2.60) plotted against the angle of the applied magnetic field to the multilayer plane. (c) and (d) show the corresponding variations in intensities from the difference spectra: (c) $g = 4.7$ (○) (S.E.M range 0.21–1.24), $g = 4.4$ (△) (0.46–1.15), $g = 4.2$ (◇) (0.62–3.35) and $g = 3.9$ (▽) (0.27–0.89). (d) $g = 3$ (○) (0.87–1.47) and $g = 2.25$ (△)(0.37–2.48).

The mosaic spread of the samples varies from 20–40%, as judged from the orientation dependence of the $g = 3$ signal (Figs. 1 and 2). This is comparable with previous studies [8,17], given that the EPR mosaic spread measurement is always somewhat (30–50%) greater than that observed in X-ray studies, since the EPR estimate covers the whole of the sample, including unoriented edges [8].

### *2.3. Electron paramagnetic resonance spectroscopy*

EPR spectra were obtained using a Bruker ER200D spectrometer interfaced to a ESP3220 computer (Bruker Analytische Messtechnik, Silberstreifen, W-7512, Rheinstetten 4, Germany) equipped with a variable temperature cryostat and liquid helium transfer line (Oxford Instruments, Osney Mead, Oxford, England). The angle between the plane of the sample sheet and the applied magnetic field was measured by a goniometer.

## 3. Results and discussion

The following resonances were observed in the spectra obtained from oriented multilayers of the azide–NO complex of cytochrome $aa_3$: $g = 6.0$ (high-spin ferric haem); $g = 3.0$ and $g = 2.25$ (low-spin ferric haem); $g = 4.7$ to 3.9 (azide–NO compound, $\Delta M_s = 2$ signal) and $g = 2.6$ (azide–NO compound, part of the $\Delta M_s = 1$ signal); resonances around $g' = 3.5$ and $g' = 11$ (integer spin complex) and $g = 4.3$ (adventitious iron).

Fig. 1a shows the spectra of oriented multilayers of cytochrome $aa_3$, predominantly as the azide–NO complex, with the applied magnetic field at angles between $-15°$ and $105°$ to the plane of the membrane. $0°$ indicates the field parallel to the membrane

plane and 90° indicates the field perpendicular to the membrane plane. Resonances at $g = 6.0$ due to high-spin ferric haem, and signals at $g = 3.0$ and $g = 2.25$ due to low-spin ferric haem are clearly visible. A complex of signals between $g = 4.7$ and $g = 4$ is due to the azide–NO complex. It is overlapped by the spectrum of the middle Kramers' doublet of rhombic high-spin ferric iron at $g = 4.3$; a small amount of adventitious iron can interfere here because of its isotropic $g$ tensor and high transition probability [19]. In addition, there are broad resonances at $g = 2.6$, due to $\Delta M_S = 1$ transitions within the triplet of the azide–NO compound, and unassigned integer–spin resonances at around $g' = 3.5$. In some samples, a broad signal at low field, with a $g'$ value at its inflexion point of 11 was observed, this is also due to an integer–spin complex. Fig. 1b shows difference spectra of multilayers with the applied magnetic field at angles between $-15°$ and 105° to the membrane plane; each difference spectrum is the spectrum at 0° subtracted from the spectrum at each angle of the applied field. The difference spectra have the advantage of removing unoriented signals, in particular the $g = 4.3$ signal (isotropic Fe(III)) which overlaps the region of interest.

The magnitude of the $g = 6.0$ signal is small, as expected from the ligand and redox state of the sample. It is apparent from Fig. 1a that the residual $g = 6.0$ signal is most intense with the applied magnetic field perpendicular to the plane of the membranes (90°). The magnitudes of the low-spin haem signals at $g = 3.0$ and $g = 2.2$ are greater, their angular dependencies giving maximal signal with the applied magnetic field parallel to and at 60° to the plane of the membranes respectively (Fig. 1a). These orientations accord with the observations of Blum et al. [8], and are probably determined by the orientation of the planes of the axial histidylimidazole ligands of the $a_3$ and $a$ ferrihaems.

In the difference spectra (Fig. 1b), the decrease in intensity in the $g = 3.0$ signal as the angle which the applied magnetic field makes with the membrane plane increases is shown as a trough of increasing intensity. Similarly, the increasing troughs at $g = 4.7$, 4.4, 4.2 and 4.0 as the applied magnetic field approaches an angle of 90° to the membrane plane shows that the azide–NO half field signals are maximal at 0°. The resonance at around $g = 2.6$, corresponding to part of the $\Delta M_S = 1$ signal of the azide–NO compound, which extends through the $g = 2$ region, has a more subtle orientation dependence. This signal is weak since it is broad and because the principal magnetic axes of the system do not line up with the plane and normal of the membrane. Whilst the intensity of the $\Delta M_S = 1$ triplet transitions is less orientation dependent than the intensities of the more anisotropic $S = 1/2$ and $S = 5/2$ ferrihaem signals, it is apparent from Fig. 1b that intensity has moved in towards $g = 2$ in the spectra in which the Zeeman field is perpendicular to the membrane plane.

Fig. 2 shows the data presented in Fig. 1 in a graphical form and confirms the orientations of the $g = 3$ and 2.2 (low-spin) resonances. These signals serve as intrinsic controls for the measurement of the angle of the applied magnetic field to the membrane plane and they allow the extent of orientation of the multilayers to be assessed. The triplet signals around $g = 4$ all follow a very similar pattern of orientation. However, it is necessary to look at the difference spectra to see this in the case of the $g = 4.2$ signal since the large underlying signal from unoriented non-haem iron associated with the membrane otherwise obscures the angular dependence of this signal (compare Fig. 2a and c). All the triplet signals are maximal with the applied magnetic field at 0°, falling at higher angles with a small increase with the applied field at 90°.

Stevens et al. [9] had proposed that the 'NO–azide' triplet state was formed by dipolar coupling between the ferrohaem $a_3$-NO complex ($S = 1/2$) and the cupric $Cu_B$–azide complex ($S = 1/2$); $D$ was inferred to be $\sim 500$ G, and the distance between the metal centres was estimated as about 5 Å. The recently reported crystal structures of cytochrome oxidases from *Paracoccus* and ox-heart mitochondria confirm that the Cu–Fe distance is about 5 Å, and indicate that the orientation of the Cu–Fe vector is no more than 20° out of the membrane plane. In the *Paracoccus* structure, electron density observed between the iron and copper atoms in the binuclear site was attributed to either water or azide (present as an antimicrobial) in this position; under the conditions of crystalization, we would expect the copper to bind azide.

In the ferrohaem $a_3$–NO cupric $Cu_B$–azide complex, NO must be bound to the haem face oriented

toward $Cu_B$ because of the location of the histidyl imidazole ligand. However, azide may be bound facing away from the haem in this complex, since the polypeptide supplies only three ligands which appear to be nearly coplanar with the copper itself [1]. Unpaired electron density in the ferrohaem $a_3$–NO species will be spread primarily over the iron and NO moieties; from the standpoint of dipolar interactions, the $r^{-3}$ weighting will therefore produce a dipolar coupling characteristic of the Cu–NO distance rather than the Cu–Fe distance. Since the NO is bound in a bent configuration, deviations from cylindrical symmetry will make the point dipole approximation poor, resulting in a relatively large $E$ term in the dipolar Hamiltonian.

Within these constraints, we find that the triplet model can account for the orientation of the triplet resonances rather well. The orientation dependence of the odd electron resonances from ferrihaem arises primarily from $g$ tensor anisotropy rather than transition probability effects, and results in changes in the position of intensity in the spectra rather than loss or gain of intensity; see, for example, the relationship between the features at $g = 3$ and $g = 2.2$ from low spin ferrihaem in Fig. 1a. The orientation dependence of the half field signals, on the other hand, arises almost entirely from transition probability effects. The transition probability of the $\Delta M_S = 1$ transitions is almost orientation independent. The orientation dependence of these signals is manifested through field position. For small $E$, the splitting of the two $\Delta M_S = 1$ transitions is $\pm 2D$ for $H$ along $z$ and $\pm D$ for $H$ in the $xy$ plane. An example of this kind is provided by the dipolar coupled ubisemiquinone pair associated with succinate ubiquinone reductase [20], in which the observed orientation dependence of the splitting is caused by the alignment of the ubiquinone–ubiquinone vector with the membrane normal. This caused the two outer lines to appear when the Zeeman field is aligned with the membrane normal.

In the present case, it is clear from the data that the $z$ axis of the system, here identified with the interspin vector, does not correspond to the membrane normal, and in fact must lie closer to the membrane plane. This is readily rationalized in terms of the available crystal structure. If the $z$ axis were along or near the normal, we would be able to observe a strong orientation dependence of the $\Delta M_S = 1$ transitions, since the unique orientation giving a 2D splitting would coincide with the unique molecular orientation along the normal. Compared to the ubiquinone–ubiquinone system described above, the system is further from axial symmetry, and $g$ tensor anisotropy is superimposed upon the anisotropy of the dipolar term. Since the orientation of the $g$ tensors of the two interacting species are unknown, the orientation dependence of the signals in this region is difficult to interpret in detail.

The position of the $\Delta M_S = 2$ lines has only a second order dependence on $D$ and $E$, the dipolar zero field splitting parameters, since the measurements were performed under conditions where the Zeeman splitting between the $+1$ and $-1$ states is $h\nu$. $D$ is equivalent to approximately 0.1 $h\nu$ [9]; $E$ is at most $1/3$ $D$ and can be much smaller, so that we are working in the strong (Zeeman) field range with respect to terms in $E$. The intensity of the transition is, on the other hand, highly orientation dependent. The transverse mode transition is first order forbidden at all orientations in a strong Zeeman field. For a coupled system with low Zeeman anisotropy, second order terms in $D$ and $E$ contribute intensity to the half field lines [21]. Although the Zeeman terms for the ferric paramagnetic states of cytochrome $a_3$ are highly anisotropic, in this state the $g$ tensor of the ferrous NO complex has only 5–10% anisotropy [22]. We expect the anisotropy of the cupric ion to be similar. $D$ is $3/4\mu_1\,\mu_2\langle(r^2 - z^2)/r^5\rangle$, while $E$ is $3/4\mu_1\,\mu_2\langle(y^2 - x^2)/r^5\rangle$, where the $\mu$ are the magnetic moments of the two spins, $r$ is the interspin vector, and the pointed brackets denote averages over the electron distribution. Since the unpaired electron associated with the haem–NO complex is delocalized over a bent system comparable in extent to the interspin distance, there is not even approximate cylindrical symmetry and we expect $E$ to be dominated by the electron distribution rather than the Zeeman terms. The half-field transitions are primarily parallel-polarized, but transverse mode signals can be observed at orientations where both the r.f. and Zeeman fields have components along $x$, $y$ or $z$. In the oriented system studied here, restricted ranges of the orientations of the molecular axis with respect to both the Zeeman and r.f. fields are available compared to solution. In solution, all possible orientations of these

fields are present, subject only to the constraint that each molecule is subject to a Zeeman field 90° from the r.f. field. In a multilayer experiment, the experimental design forces the r.f. field to always lie in the plane of the multilayer, and hence of the individual membranes. All possible orientations of the triplet about the normal are present, so that for each orientation of the Zeeman field with respect to the membranes some molecules will have the r.f. field aligned with each in plane direction (Fig. 3).

In the transverse mode, each Zeeman field orientation in the molecular coordinate system thus corresponds to a unique perpendicular r.f. field orientation, except when the Zeeman field is along the membrane normal. If the molecular $z$ axis were along the membrane plane, the maximum half field intensity would be observed with the Zeeman field in the in-plane orientation, since then orientations would be present in which both the r.f. and Zeeman fields had components along both $x$ and $y$. With the $z$ axis in or near the membrane plane, the maximum intensity would be present at intermediate angles close to 45°, since then the Zeeman and r.f. fields would have components along either $x$ or $y$.

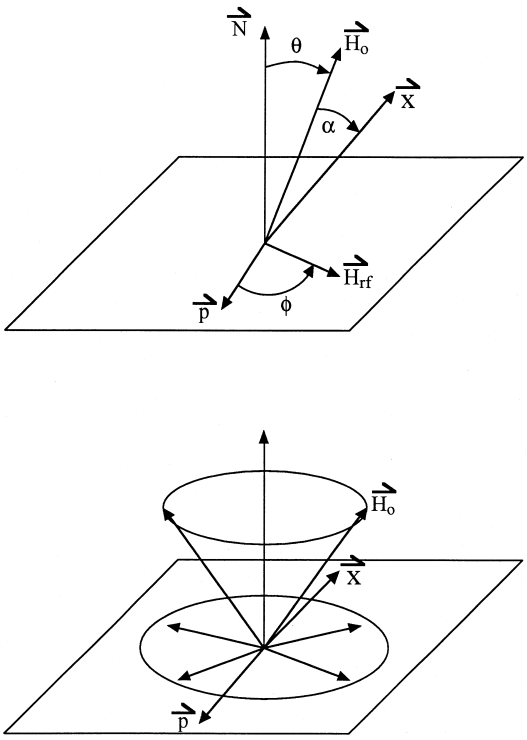


Fig. 3. Top: Orientation of $H_0$ and $H_{rf}$ with respect to a single molecule in a multilayer. $p$ is the projection of the molecular $yz$ plane in the membrane, $n$ is the membrane normal and $p \perp x$, $H_0 \perp H_{rf}$. Bottom: Cone of possible orientations in molecular coordinate system for a single value of $\theta$, with the corresponding disc of $H_{rf}$ orientations.

Since our results suggest that the model of Stevens et al. [9] for the coupled azide–NO system is essentially correct, it is of interest to compare the available X-ray data with constraints placed on the system by spin-coupling. Information from several sources can be combined to construct a model of the bi-liganded state. The approximate structures of the unliganded binuclear site and of the azide complex are available from X-ray data [1]. The azide appears to be bound between the metal ions in this case; under corresponding conditions in solution, the azide would be bound to the copper and not to the iron, since the haem is high spin [11].

From previous orientation work, we know that the haem plane is perpendicular to the membrane plane; this has been confirmed by X-ray diffraction. X-ray results established a haem–Cu distance of 4.75 Å. Barlow and Erecinska [23] measured the orientation of the NO bond in the ferrohaem–NO complex; they found it was 45° from the membrane plane. Since the Fe–N–O bond angle is typically around 140°, the Fe–N–O plane was perpendicular to the membrane plane. In the azide–NO complex, the ferrohaem binds NO in the space between the metal ions. The orientation of the NO may be similar, but this has not yet been established. It is likely that the azide coordinating the copper in this complex is oriented away from the haem, in contrast to the azide complex in the absence of NO, since azide is a long rigid ligand which would otherwise interact sterically with the NO bound by ferrohaem. The coordination of the copper by only three polypeptide-derived ligands which are nearly coplanar with the copper makes the possibility of two alternative binding modes feasible (Fig. 4). It is of considerable potential significance that the existence of two such alternative ligand binding modes is suggested by the data, and that the switch which selects the mode appears to be the ligation state of the adjacent haem, since similar mechanisms have been suggested to lie behind the proton translocation mechanism of the enzyme [24,25]. We hope to provide additional information by conducting parallel mode experiments, which

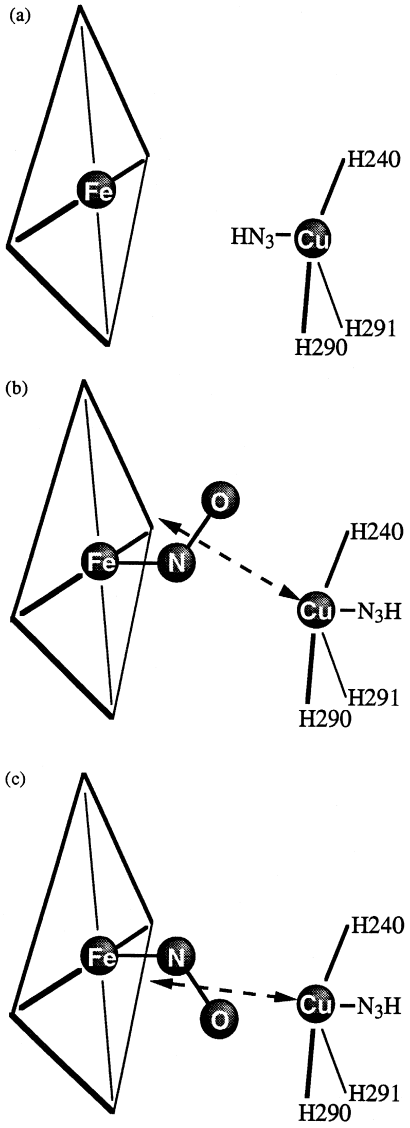


Fig. 4. Model of the binuclear site of cytochrome $aa_3$ including haem–copper vector data. (a) Azide alone bound. (b), (c) Alternative orientations of bound NO in the presence of azide, showing the approximate interspin vector (dotted line). The metal–metal distance is approximately 5 Å and the copper is displaced approximately 1 Å along the membrane normal relative to the iron. Note that the haem ring and copper ligands are not to scale.

would allow us to vary the orientations of $H_o$ and $H_{rf}$ simultaneously.

## Acknowledgements

DJBH and WJI acknowledge the support of BBSRC project grant GR/J 33142.

## References

[1] T. Tsukihara, H. Aoyama, E. Yamashita, T. Tomizaki, H. Yamaguchi, K. Shinzawa-Itoh, R. Nakashima, R. Yaono, S. Yoshikawa, Science 269 (1995) 1069–1074.
[2] S. Iwata, C. Ostermeier, B. Ludwig, H. Michel, Nature 376 (1995) 660–669.
[3] P. Lappalainen, M. Saraste, Biochim. Biophys. Acta 1147 (1994) 222–225.
[4] W.R. Hagen, Biochim. Biophys. Acta 708 (1982) 82–98.
[5] V. Chepuri, R.B. Gennis, J. Biol. Chem. 265 (1990) 12978–12986.
[6] J.P. Hosler, S. Ferguson-Miller, M.W. Calhoun, J.W. Thomas, J.J. Hill, L.J. Lemieux, J. Ma, C. Georgiou, J. Fetter, J.P. Shapleigh, M.M.J. Tecklenburg, G.T. Babcock, R.B. Gennis, J. Bioenerg. Biomembr. 25 (1993) 121–136.
[7] S. Brown, J.N. Rumbley, A.J. Moody, J.W. Thomas, R.B. Gennis, P.R. Rich, Biochim. Biophys. Acta 1183, 521–532.
[8] H. Blum, H.J. Harmon, J.J. Leigh, J.C. Salerno, B. Chance, Biochim. Biophys. Acta 502 (1978) 1–10.
[9] T.H. Stevens, G.W. Brudvig, D.F. Bocian, S.I. Chan, Proc. Natl. Acad. Sci. U.S.A. 76 (1979) 3320–3324.
[10] G.W. Brudvig, T.H. Stevens, S.I. Chan, Biochemistry 19 (1980) 5275–5285.
[11] W.J. Ingledew, J. Horrocks, J.C. Salerno, Eur. J. Biochem. 212 (1993) 657–664.
[12] M.W. Calhoun, R.B. Gennis, W.J. Ingledew, J.C. Salerno, Biochim. Biophys. Acta 1206 (1994) 143–154.
[13] D.E. Green, D.M. Ziegler, Meth. Enzymol 6 (1963) 416–424.
[14] J.C. Salerno, W.J. Ingledew, Eur. J. Biochem. 198 (1991) 789–792.
[15] J.K. Blasie, M. Erecinska, J.S. Leigh, S. Samuels, Biophys. J. 17 (1977) 63a.
[16] J.S. Leigh, H.J. Harmon, Biophys. J. 17 (1977) 251a.
[17] J.K. Blasie, M. Erecinska, S. Samuels, J.S. Leigh, Biochim. Biohys. Acta 501 (1978) 33–52.
[18] W.J. Ingledew, R.A. Rothery, R.B. Gennis, J.C. Salerno, Biochem. J. 282 (1992) 255–259.
[19] W.E. Blumberg, in: A. Ehrenberg, B.G. Malmstrom, T. Vanngard (Eds.), Magnetic Resonance in Biological Systems, Pergamon Press, Oxford, 1967, pp. 119–133.
[20] J.C. Salerno, H. Blum, T. Ohnishi, Biochim. Biophys. Acta 547 (1978) 270–281.
[21] J.H. van der Waals, M.S. de Groot, Mol. Phys. 2 (1959) 333–340.
[22] M.F.J. Blokzijl-Homan, B.F. Van Gelder, Biochim. Biophys. Acta 234 (1971) 493–498.
[23] C. Barlow, M. Erecinska, FEBS Lett. 98 (1978) 9–12.
[24] P.R. Rich, Aust. J. Plant Physiol. 22 (1995) 479–486.
[25] M. Wikström, A. Bogachev, M. Finel, J.E. Morgan, A. Puustinen, M. Raitio, M. Verkhovskaya, M.I. Verkhovsky, Biochim. Biophys. Acta 1187 (1994) 106–111.